Quaternary Science Reviews 294 (2022) 107762

Contents lists available at ScienceDirect

Quaternary Science Reviews

journal homepage: www.elsevier.com/locate/quascirev

Intensification of ENSO frequency drives forest disturbance in the andes during the holocene

K. Hagemans [a], D.H. Urrego [b], W.D. Gosling [c], D.T. Rodbell [d], F. Wagner-Cremer [a], T.H. Donders [a, *]

[a] Department of Physical Geography, Faculty of Geosciences, Utrecht University, Utrecht, Netherlands
[b] Geography, College of Life and Environmental Sciences, University of Exeter, Exeter, United Kingdom
[c] Institute for Biodiversity and Ecosystem Dynamics, University of Amsterdam, Amsterdam, the Netherlands
[d] Geology Department, Union College, Schenectady, NY, USA

ARTICLE INFO

Article history:
Received 31 May 2022
Received in revised form
7 September 2022
Accepted 8 September 2022
Available online 17 September 2022

Handling editor. Claudio Latorre

Keywords:
El niño
Andes
Pollen
Alnus
Landslides

ABSTRACT

The biodiverse montane forests of the tropical Andes are today frequently disturbed by rainfall-driven mass movements which occur mostly during extreme El Niño events. Over the coming decades these events are projected to double under the 1.5 °C global warming scenario. The consequent increased rainfall and mass movement events likely present an elevated risk to millions of people living in the Andes. However, the impact of more frequent rainfall extremes remains unclear due to a lack of studies that directly link past changes in El Niño-Southern Oscillation (ENSO) frequency to forest and landscape disturbance patterns. Here, we present the first Holocene palaeoecological record from Laguna Pallcacocha, southern Ecuador, a key site for El Niño reconstructions. We demonstrate that for the past 10,000 years plant taxa indicative of recolonization – such as *Alnus acuminata* – covary with El Niño-induced flood layers in the lake. An amplified forest disturbance pattern is observed in the late Holocene, suggesting enhanced slope instability following deforestation. The temporal pattern is not explained by tree line fluctuations or human impact, while the latter does amplify the impact of ENSO on landscape disturbance. Spatial correlations between modern ENSO and precipitation are consistent with a regional comparison of Holocene records of landscape disturbance. Our results indicate that climate extremes, such as those associated with future intensification of El Niño, combined with ongoing land use change will increase the frequency of mass movements elevating risks for millions of people in the Andes.

1. Introduction

The montane forests of the western Tropical Andes are a biodiversity hotspot and contain some of the most threatened habitats on the planet. Exceptional levels of plant endemism (Myers et al., 2000; Pérez-Escobar et al., 2022) combined with narrow altitudinal habitat ranges make these forests sensitive to disturbance and climate change (Foster, 2001). Small-scale yet severe mass movements, that include landslides and debris flows, occur frequently on steep slopes in tropical montane forests (Crausbay and Martin, 2016; Muenchow et al., 2012; Richter, 2009). Triggered by intense rainfall (Clark et al., 2016) and occasional earthquakes (Crausbay and Martin, 2016), mass movements create gaps in the forest canopy and remove nutrient-rich soils (Crausbay and Martin, 2016). As a result, mass movements provide niches for rare and early-successional species (Crausbay and Martin, 2016) and contribute to vegetation heterogeneity and species diversity in Andean forests (Crausbay and Martin, 2016; Ohl and Bussmann, 2004; Richter, 2009). Landslides and debris flows are also a pervasive geohazard with 52% of Andean people at risk (Comunidad Andina, 2009), and their occurrence may increase in likelihood under climate warming.

Rainfall variability in the western Tropical Andes is influenced by the El Niño-Southern Oscillation (ENSO) (Vuille et al., 2000). Every 2–7 years El Niño events amplify atmospheric convection causing regional warming and intense rainfall events along tropical western Andean slopes (Kiefer and Karamperidou, 2019; McPhaden et al., 2006; Vuille et al., 2000). High-resolution meteorology shows that rainfall events that exceed landslide threshold levels are primarily derived from the Pacific (Hagemans et al., 2021) and occur

* Corresponding author.
E-mail address: t.h.donders@uu.nl (T.H. Donders).

https://doi.org/10.1016/j.quascirev.2022.107762

during Eastern Pacific and Coastal Pacific El Niño events (Kiefer and Karamperidou, 2019) (Fig. S3). Twenty first century climate projections estimate doubling of extreme El Niño frequency at 1.5 °C climate warming and continued increase in occurrence after climate warming stabilization (Wang et al., 2017). The IPCC Sixth Assessment Report (AR6) reaffirmed the projected ENSO-tied rainfall intensity (IPCC et al., 2021), although for the projected sea surface temperature (SST) change that would drive El Niño rainfall variability the AR6 reports no model consensus. In a critical analysis of this conclusion Cai et al. (2022) demonstrate, using the Coupled Model Intercomparison Project (CIMP6) projections, a robust 20th to 21st century SST increase that sustains the earlier projections of Wang et al. (2017) with doubling of future extreme El Niño events and associated increased rainfall variability.

Already, the impact of climate warming on Andean ecosystems is evident in the upslope migration of tree species in Peru (Feeley et al., 2011) and compositional shifts and range retractions in Colombia (Duque et al., 2015). However, to what extent a warming-induced intensification in El Niño frequency will impact the (in) stability of tropical Andean slopes and composition of forests remains unknown. Monitoring of ENSO over recent decades provides detailed insights into system function under the current climate configuration, but is of insufficient length to document forest (in) stability over timescales that capture the projected future ENSO frequency change. Studying past forest (in)stability, when El Niño frequency was similar or higher than present day, can shed light on the long-term (in)stability of Andean forests for the future.

Laguna Pallcacocha (2°46′S, 79°14′W; 4050 m a.s.l.; El Cajas National Park [ECNP]) yielded the important terrestrial record of El Niño-induced rainfall variability during the past 10,000 years (Moy et al., 2002; Rodbell et al., 1999) (Fig. 1). Recent work demonstrated that Pacific-sourced rainstorm events, associated with coastal El Niños, trigger mass movements in the Pallcacocha catchment. These mass movements deposit clastic layers in the lake at frequencies that fall into the typical El Niño frequency band (Hagemans et al., 2021). This new insight answers recent questions (Schneider et al., 2018) regarding the original interpretation of the drivers of this laminae record (Moy et al., 2002; Rodbell et al., 1999). The Holocene laminae frequency pattern shows a gradual increase of El Niño events, superimposed by millennial-scale variations (Moy et al., 2002; Rodbell et al., 1999) (Fig. 2). The change from lower El Niño frequency in the early and mid-Holocene (Moy et al., 2002; Rodbell et al., 1999) to higher and more variable El Niño frequencies in the late Holocene is recognized in marine and terrestrial records globally (e.g. Donders et al., 2008; Thompson et al., 2017; White et al., 2018). The importance of original Pallcacocha laminae record warrants further investigation on the reginal consistency and consequences of the ENSO dynamics in the Andes. Here, we apply pollen and microcharcoal analyses on the organic fraction of the Pallcacocha sediments to reconstruct Holocene vegetation history and derive forest disturbance patterns and couple them to the inorganic laminae deposition evolution. Modern pollen samples from ECNP demonstrate that pollen from montane forests in a ~40 km radius around Pallcacocha are recorded in the lake sediments (Hagemans et al., 2019). Based on these calibrations and ecological observations (Hagemans et al., 2019; Paolini et al., 2005), we use characteristic pollen types to determine changes in upper forest line, post-disturbance recolonization, páramo (alpine Andean grasslands) and anthropogenic activity on decadal to centennial resolution. Our palaeoecological reconstruction couples regional-scale forest disturbance and (in)stability of the tropical Andean landscape via the iconic paleo-El Niño laminae record from Pallcacocha to El Niño-induced rainfall events.

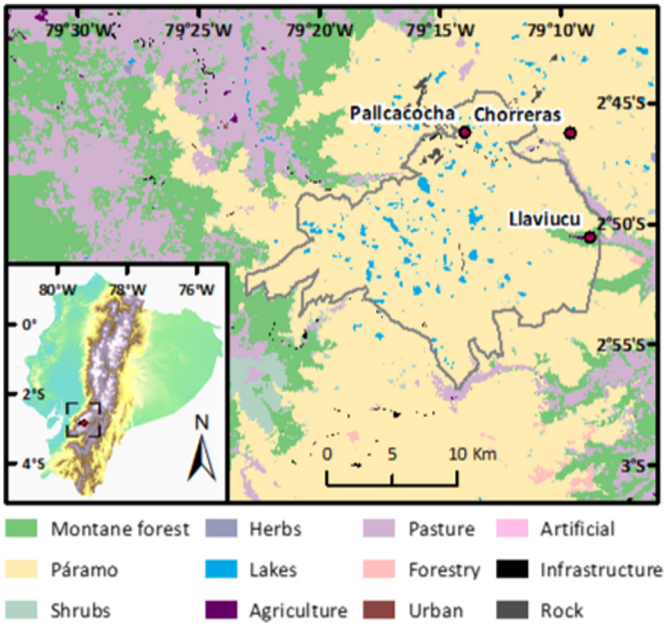

Fig. 1. Vegetation types in the vicinity of Laguna Pallcacocha and other lakes mentioned in section 4.1. Laguna Pallcacocha and nearby Laguna Chorreras are situated in the grass páramo. Laguna Llaviucu is situated in a valley covered with montane forest. Páramo dominates the El Cajas National Park. Montane forests cover the slopes of the inter-Andean valley and the Pacific-side of the western Andean Cordillera of Ecuador. The grey line represents the border of the El Cajas National Park. Vegetation map was provided by Ministerio del Ambiente Ecuador (2014). Inset: Topography of Ecuador and location of study site. Elevations are based on SRTM data provided by USGS (2014). Laguna Pallcacocha is situated on the western Andean cordillera.

2. Material and methods

A 9-m composite sediment core from Laguna Pallcacocha, retrieved in 1999 (Moy et al., 2002), was sampled at 5-cm intervals for palynological analyses and micro-charcoal processing. The 0.3 cc samples were spiked with 4 mL *Lycopodium clavatum* solution (i.e., ~8339 spores) and processed following standard palynological protocols (Faegri and Iversen, 1989). The sediment samples were floated over sodium polytungstate (density = 2.0) to remove minerals. Pollen was counted to a minimum of 300 terrestrial pollen grains per sample with a Leica DM2500 light microscope at 400× magnification. Pollen types were identified to the lowest taxonomic level possible following descriptions by Hooghiemstra (1984), and by comparison with the reference collections at the University of Amsterdam and Utrecht University. *A. acuminata* pollen, non-pollen palynomorphs (NPPs) and spores were excluded from the pollen sum shown in Fig. 2, but *A. acuminata* is included in the sum for the regional comparison (Fig. 4). Fungal NPPs were identified following descriptions by van Geel et al. (2011). Micro-charcoal particle number and surface area and *L. clavatum* occurrences were recorded using digital image analysis in ImageJ (Schneider et al., 2012). Slides were digitized microscopic at 200× optical magnification using a Leica DM6000 B automated-stage microscope. Imaging was carried out with extended focus using at 4 z-levels over 16 μm vertical distance with the Leica LAS 4.13 software equipped with Power Mosaic plus. Particle detection of the resulting composite images in ImageJ was set with a minimum threshold of 10 μm^2 and color detection ranges to; hue 90–180, brightness 0–50 and saturation 0–255. Particle circularity was set between 0.0 and 0.5. Estimates of total micro-charcoal and pollen influx were based on *Lycopodium clavatum* added per 1 cc of sediment. Statistically significant pollen assemblage zones were established using the CONISS (Constrained Incremental Sum of

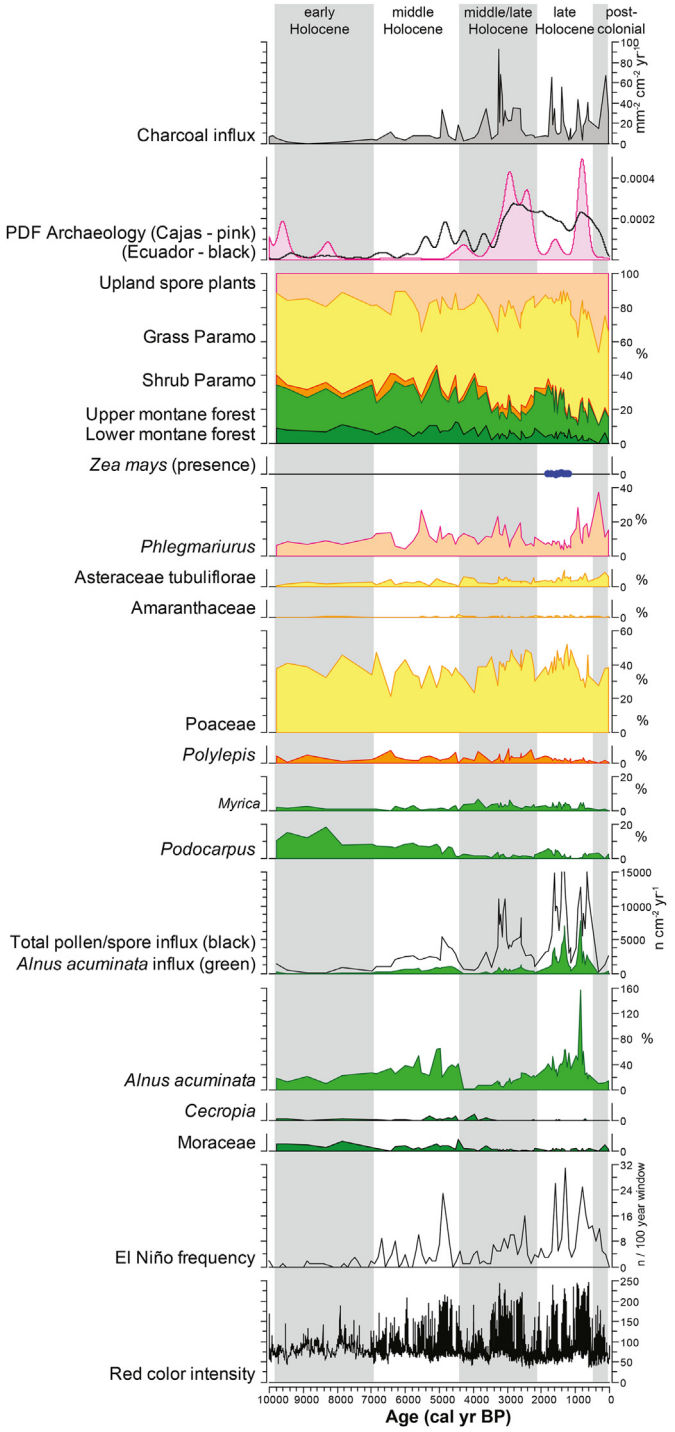

Fig. 2. Palaeoecological proxy diagram from Laguna Pallcacocha. The red color intensity and El Niño event frequencies are based on the light-colored laminations in the sediments (Moy et al., 2002; Rodbell et al., 1999). *Alnus acuminata* is a pioneering taxon in montane forests and indicative for slope destabilization and forest disturbance. Pollen abundance of up to 25% for Podocarpus spp. and 7% for Moraceae indicate local montane forest near L. Pallcacocha in the early Holocene. Poaceae and Asteraceae represent the abundance of grass-páramo vegetation which increases in the late Holocene. *Polylepis* present the subpáramo forest-grassland ecotone. Probability density functions (PDF) are based on archaeological ^{14}C dates (n = 27 in a 60-km radius around L. Pallcacocha, pink curve; all Ecuadorian ages, black line, n = 545) from South American human demography reconstructions (Goldberg et al., 2016). Blue symbols represent the presence of *Zea mays* pollen grains (<1%) in the Pallcacocha sediment record.

Squares) option with square-root transformation in Tilia (Grimm, 1987). A ^{14}C and tephra-based chronology for the core was previously established and published (Moy et al., 2002; Rodbell et al., 2002, 1999) which for reasons of consistency with the laminae frequency record we used unaltered. Regional pollen data (Fig. 4) represent available Holocene upland records in the Neotoma Paleoecology Database (http://www.neotomadb.org) (Williams et al., 2018). Probability density functions of archaeological artefacts were based on the South-American database of archaeological ^{14}C dates and human demography (Goldberg et al., 2016) and calculated with the statistical package Bchron (Haslett and Parnell, 2008) in R. To estimate mass movement density under varying El Niño regimes we first defined 5 classes: 0–5, 5–10, 10–15, 15–20 and > 20 El Niño events per 100 years as recorded in the sediments from L. Pallcacocha. We then calculated the average pollen influx of *A. acuminata* (grains cm^{-3} yr^{-1}) for those classes (Fig. 5). Modern day analyses in RBSF indicate a mass movement density of 19 slides km^{-2} per 50 years (Muenchow et al., 2012), while modern pollen samples demonstrate that in the past 50 years the average pollen influx of *A. acuminata* is ~1088 grains cm^{2} yr^{-1}. Projection of this data on the relation between *A. acuminata* influx and El Niño frequencies from Pallcacocha gives a first order estimate of mass movement density over the Holocene. All maps presented were configured with ArcMap software.

3. Results

The early Holocene (~10,000–7000 calibrated years before present, cal. yr BP) section of the L. Pallcacocha pollen record is characterized by assemblages indicative of moist montane forest (Fig. 2). During this period *Podocarpus* spp. and Moraceae reached their maximum abundance, 25% and 7% respectively. The *Alnus acuminata* abundance initially was relatively low and invariable. They are derived from the montane forest at lower elevation and therefore *A. acuminata* abundances in Fig. 2 were calculated outside the pollen percentage sum (see section 4.1). Alternatively, pollen influx data – based on counts of exotic marker grains, known sample volumes and sediment accumulation rates (grains cm^{3} yr^{-1}) (Stockmarr, 1971) – are unaffected by closed-sum effects and better highlight phases of enhanced pollen deposition in this setting. Low and stable influx and relative abundance values of *A. acuminata* pollen during the early Holocene are notable given the overall high abundance of other arboreal taxa.

The mid-Holocene (7000-4500 cal yr BP) was marked by a decrease in *Podocarpus* spp. to 9% and an increase in both *A. acuminata* influx and relative abundances, concurrent with enhanced frequencies of clastic laminae deposition (Fig. 2). Pollen of Amaranthaceae were present in very low numbers (Fig. 2) and, as expected at this elevation, the record shows little indication for extensive local on-site cultivation (e.g., *Zea mays*), extensive fire, or high density continuous human occupation (Goldberg et al., 2016). This suggest that the local vegetation record has little anthropogenic bias, but at a supra-regional scale humans were likely active given the consistent increases in the archaeological settlement density after 3500 cal yr BP in Ecuador (Fig. 2) (Goldberg et al., 2016).

The mid-to late Holocene (4500 - 2100 cal yr BP) showed a further, sharp decline in *Podocarpus* spp. accompanied with an increase of local páramo taxa (Fig. S1). Influx of *A. acuminata* pollen decreased between ~4500 and 4000 cal yr BP, when recorded El Niño events in the flood layer record of the lake declined in frequency. Micro-charcoal became abundant ~3600 cal yr BP, but declined again shortly after and remained low until ~120 cal yr BP The late Holocene zone (2100 - 400 cal yr BP) exhibited a highly similar pattern between high influx of *A. acuminata* pollen and

recorded El Niño events in the flood layer record of the lake; both reached maximum values at ~1300 and ~800 cal yr BP. During this period, a decline in *Polylepis* spp., the first occurrence of *Z. mays* ~1500 cal yr BP and expansion of human settlement occurred in the region (Fig. S2). From 400 cal yr BP to modern times reduced influx of *A. acuminata* pollen mirrored the decline in laminae deposition in the lake, while Poaceae and Asteraceae expanded. The total pollen accumulation rate mirrors the high *Alnus* influx phases. Except for the 3500 - 2500 cal yr BP period where the laminae record shows that ENSO frequencies are at intermediate levels other upper forest taxa (mostly *Myrica*, *Podocarpus, Polylepis)* show a higher influx relative to *Alnus.*

4. Discussion

4.1. El Niño-driven forest disturbance

The conspicuous variability of *A. acuminata* at L. Pallcacocha indicates highly variable forest dynamics during the Holocene (Fig. 2) instead of upslope Andean forest migration. *A. acuminata* is a pioneer species in montane forests ~1500–3400 m asl and is common in marshy areas, river beds and on post-mass movement soils (Marchant et al., 2002; Paolini et al., 2005; Weng et al., 2004a). The expansion of *A. acuminata* in the Holocene has previously been linked to an upslope migration of the montane forest in response to temperature increase (Weng et al., 2004a). However, such interpretations are generally based on surface calibrations derived from moss polsters (Olivera et al., 2009; Urrego et al., 2011b; Weng et al., 2004b), soil samples (Reese and Liu, 2005; Weng et al., 2004b) or pollen traps (Niemann et al., 2010; Olivera et al., 2009), while reconstructions of past vegetation and climate dynamics are generally based on pollen records from lake sediments (Colinvaux et al., 1997; Hansen et al., 2003; Schiferl et al., 2018; Urrego et al., 2005). Pollen rain in moss polsters and soil samples is representative of local vegetation present within a few meters, while lake sediment samples from páramo lakes such as L. Pallcacocha represent regional vegetation of up to 40 km distance (Hagemans et al., 2019). These surface calibrations for Pallcacocha and neighbouring lakes have shown that *A. acuminata* is overrepresented in pollen records from páramo lakes due to upslope wind-transport and prolific pollen production by *Alnus,* and therefore does not represent local vegetation around the lake. However, the same surface calibrations show that *Podocarpus* spp. is a (more) sensitive proxy for past forest distribution than *A. acuminata* in this setting. In the Tropical Andes, *Podocarpus* spp. are large trees that form stands in the montane forests (Marchant et al., 2002) and can reach pollen percentages above 25% in lakes surrounded by montane forest in ECNP (Hagemans et al., 2019). Such pollen percentages for *Podocarpus* spp. are reached in Pallcacocha in the early Holocene, indicating that the montane forest reached its highest distribution at this time, which is consistent with other terrestrial pollen records from the region (Hansen et al., 2003; Schiferl et al., 2018; Nascimento et al., 2020). Given the continued presence of local páramo indicators like *Phlegmariurus* and *Plantago* (Fig. 2), the upper montane forest most likely did not extend above the lake elevation at 4050 m. Deltaic deposits in front of the lake (reported in Hagemans et al., 2021) contain no visible woody macrofossils or changes in peat type suggesting that, despite a higher tree line, there was no local forest presence in the Early Holocene around Pallcacocha. Such catchment changes could be significant for the likelihood of clastic laminae deposition in the lake basin, yet we do not see any evidence for this.

By the mid-Holocene (~5000 cal yr BP) *Podocarpus* spp. decreased to ~2% in L. Pallcacocha, which is comparable to the modern day pollen abundance in the lake (Hagemans et al., 2019) and indicates a downslope migration of the upper forest line to its modern day position of 3500 m asl. Increased microcharcoal abundance regionally indicates more frequent burning of the vegetation in the region at this time, which could be sign of local settlement, and likely contributed to a downslope migration of the forest (Urrego et al., 2011a). *A. acuminata* reached maximum values in the late Holocene well after the mid-Holocene downslope migration of the upper forest limit. The high abundances and influx of *A. acuminata* in the late Holocene are therefore unrelated to a temperature driven migration of the montane forest belt and must represent another aspect of Andean forest dynamics.

We propose a new interpretation for the conspicuous variability of *A. acuminata* in Pallcacocha during the Holocene, based on the regional growth pattern of *A. acuminata* related to disturbed soils and its modern pollen distribution in ECNP (Hagemans et al., 2019). Rainfall-driven landslides play a central role in the dynamics of tropical montane forests and contribute to the maintenance of vegetation heterogeneity and species richness (Crausbay and Martin, 2016; Richter, 2009). By creating gaps in the forest canopy, landslides provide niches for the recruitment and persistence of rare and early-successional species (Crausbay and Martin, 2016). Nitrogen-fixing cryptogams are usually first to colonize the nutrient poor post-landslide soils. Mosses and lichens provide a basis for the establishment of Gleicheniaceae, Asteraceae and Poaceae (Lozano et al., 2008; Richter, 2009). *Alnus acuminata* is one of the first tree species to abundantly colonize post-landslides soils (Paolini et al., 2005), because of its nitrogen-fixing capabilities and light tolerance. Melastomataceae and Piperaceae characterize secondary shrub succession and are followed by tree taxa such as Rubiaceae, Lauraceae and Myrtaceae (Richter, 2009), but these taxa produce less pollen which are less taxa specific. Its abundant pollen production and regional source area is well recorded in the open landscape (Hagemans et al., 2019), which render it a primary and extra-local indicator of vegetation regeneration after episodes of slope instability in Andean sedimentary records (Brunschön et al., 2010) (Fig. 5). Recent records of sedimentation and high-resolution rainfall records from ECNP provide a mechanistic link between clastic sedimentation from alluvial activity in the catchment of Pallcacocha and intensive rainfall events originating from the Pacific, such as those during coastal El Niños (Hagemans et al., 2021). We submit that regional-scale landscape disturbance is reflected in the variability of *A. acuminata* at Pallcacocha and is the result of increased El Niño-driven mass movements. In that view, the conspicuous variability of *A. acuminata* at Pallcacocha indicates severe and highly variable forest disturbance during the late Holocene (Fig. 2). Our surface data indicate that the influx of *A. acuminata* pollen is independent of other, local vegetation elements in ECNP and can be used to document past relative levels of forest disturbance related to mass movements. The synchrony between the *A. acuminata* pollen influx pattern and the frequency of laminae deposition (Fig. 2) thus indicates that the dynamics of local sediment deposition in Pallcacocha parallels the developments of regional scale disturbance patterns (Fig. 4).

Comparison of the observed dynamics in pollen abundance of *A. acuminata* in L. Pallcacocha to other pollen records across the Tropical Andes shows that a highly similar, largely bi-modal Holocene pattern of *Alnus* abundance is recorded some areas (Fig. 4) that, based on spatial patterns in reanalysis data, presently experience a clear climatic impact from ENSO (Fig. 3). This pattern of bimodal Holocene expansion and retraction in *A. acuminata* abundance from Pallcacocha is evident in various terrestrial pollen records across the Ecuadorian Tropical Andes (Weng et al., 2004a), such as nearby lakes Laguna Llaviucu (Colinvaux et al., 1997; Nascimento et al., 2020), Laguna Chorerras (Hansen et al., 2003) and a marine record from the Pacific Guayaquil basin (Seillès et al.,

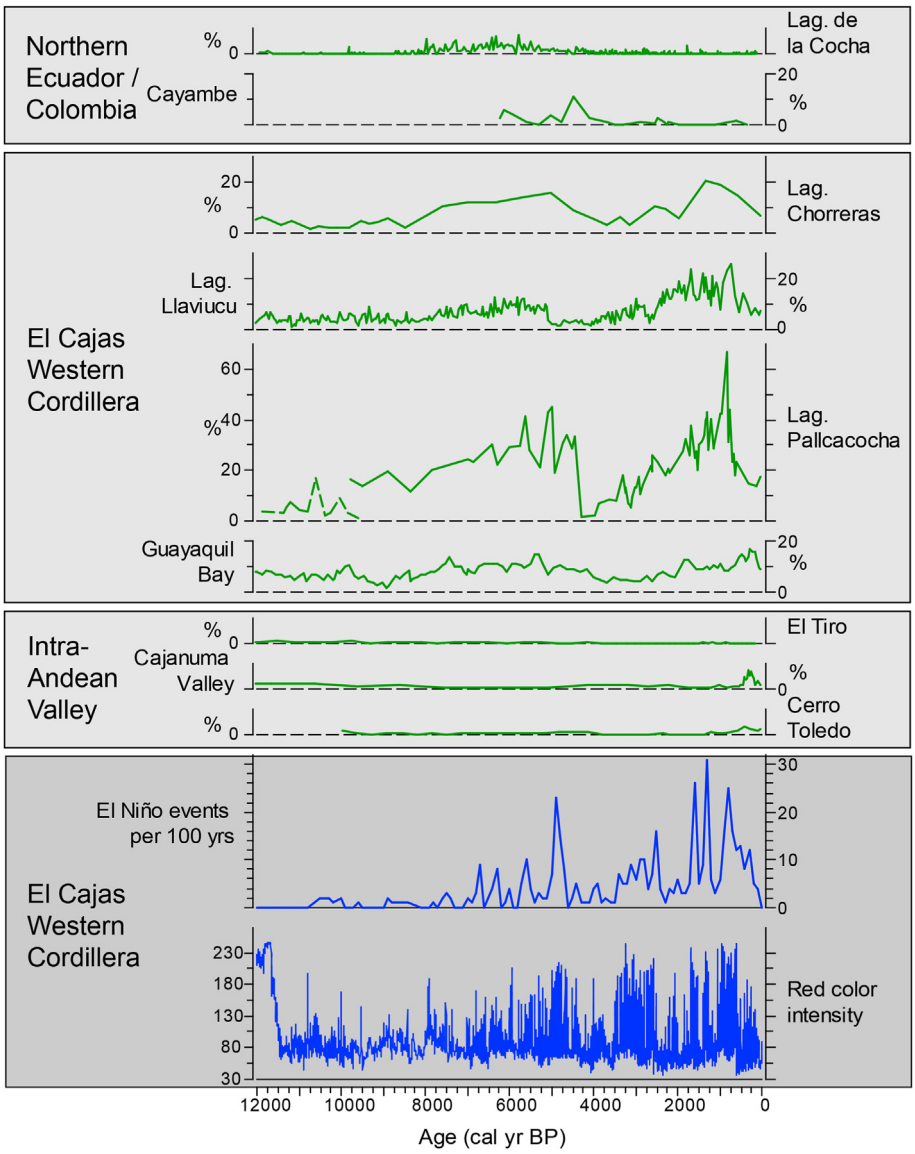

Fig. 3. High elevation sites included in the regional analysis (details see Table 1). Overlay shows correlation between November–January averaged precipitation and the NINO 1.2 index 1979–2019 for Ecuador and Southern Colombia. Correlation obtained with KNMI Climate Explorer (https://climexp.knmi.nl/start.cgi) and adjusted in ArcGis (Environmental Systems Research Institute, 2014).

2015), with a more pronounced signal in high-elevation sites (Fig. 4, Table 1). In contrast, sheltered sites situated in the inter-Andean valley (Niemann and Behling, 2008; Brunschön and Behling, 2009; Villota and Behling, 2014) or further north (Graf, 1992; González-Carranza et al., 2012, Table 1, Figs. 3 and 4) show overall much lower *A. acuminata* abundances and exhibit a clearly different temporal pattern with no late Holocene increase. All these sites presently show a weak or inverse correlation to ENSO-induced rainfall (Fig. 3). The Holocene *Alnus* patterns in the ENSO sensitive regions, while highly similar, are not identical and temporal offsets are likely related to local threshold differences in *Alnus* regrowth with regard to disturbance and variations in sediment accumulation rates between sites. Differences in radiocarbon calibration are unlikely to explain the site offsets as significant changes between successive radiocarbon calibration curves (Stuiver et al., 1998; Reimer et al., 2009, 2013) are mostly in the pre-Holocene sections. The consistency between regional records in areas with a modern-day prominent ENSO impact provides further support for a regional factor driving *A. acuminata* populations in the Tropical Andes. Mass movement occurrences in the Andes have been linked to El Niño (Comunidad Andina, 2009; Keefer et al., 2003; Moreiras, 2005; Sepúlveda et al., 2006) and in the ECNP intense rainfall events are mostly triggered by coastal El Niño events (Kiefer and Karamperidou, 2019). We infer that as rainfall anomalies triggered by Eastern Pacific and Coastal Pacific El Niño events occurred more frequently in the late Holocene, it triggered mass movement activity and subsequently provided opportunities for *A. acuminata* to expand.

The disturbance pattern is amplified in the late Holocene as people become more active in the landscape (Fig. 2), as proposed earlier by Nascimento et al. (2020). Probability density functions (PDF) based on archaeological ^{14}C dates and reconstructions of human demography within ~40 km radius (i.e. the pollen source area) of Pallcacocha indicate increases in human activity during the late Holocene (Fig. 2). Pollen records from the lower elevation Laguna Llaviucu (3150 m asl) in ECNP match the timing of

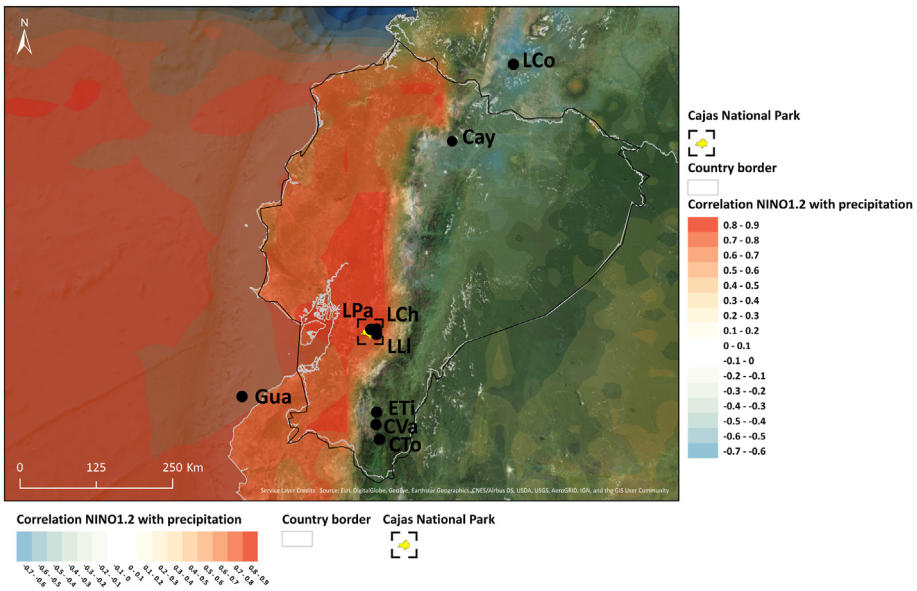

Fig. 4. Holocene dynamics in Alnus from L. Pallcacocha compared to available high elevation records from Ecuador and southern Colombia, as well as marine core M772056-2 from the Bay of Guayaquil. The red color intensity and derived El Niño event frequency are based on the same sediment core and chronology from L. Pallcacocha (Moy et al., 2002; Rodbell et al., 1999). All *A. acuminata* percentages are expressed relative to the total sum of upland herbs, shrubs and trees. See Table 1 and Fig. 3 for site details and locations relative to current ENSO climate influence. The L. Chorreras chronology has been revised based on the tephra ages from ECNP (Rodbell et al., 2002).

Fig. 5. Characteristic debris flows in the montane forest ~10 km northeast of El Cajas National Park. Photograph taken by D.T. Rodbell in July 1995.

intensification of the laminae deposition (Fig. 4), suggesting that the adoption of agricultural and pastoralist activities amplified existing ENSO signals through the increase of landscape sensitivity in the late Holocene (Nascimento et al., 2020). While the Pallcacocha data do not show clear indications for agriculture intensification (e.g., low *Zea mays*, Amaranthaceae) during the observed increases in late Holocene laminae and *A. acuminata*, more regional-scale information on the temporal patterns of habitation is required. The central Ecuadorian Azuay and Cañar provinces, in which the ECNP is located, were inhabited by the Cañari people before the Incan conquest of the region (~500 cal yr BP). The Cañari were primarily agriculturalists maintaining an intensive, irrigation-based economy in the warm low elevation valleys producing cotton and coca (Bray and Echeverría, 2018). They lived in small hamlets or individual homesteads dispersed across the landscape (Bray and Echeverría, 2018). In the ECNP and its surroundings 27 dated archaeological sites have been registered that indicate the settlement of people in the area between 3500 cal yr BP. and 500 cal yr BP (Ministerio del Ambiente del Ecuador, 2018) (Fig. 2). In Pallcacocha, the key Andean crop *Z. mays* first appeared in the record at 1800 cal yr BP. and remained consistently present in low abundances for 600 years until it disappeared at 1200 cal yr BP. (Fig. 2). Other anthropogenic indicators such as Amaranthaceae also remained low between 1800 cal yr BP and 1200 cal yr BP, while

Table 1
Site details for regional comparison of pollen records in Fig. 4

Site name	Abbreviation	Region, country	Elevation (m asl)	Habitat	Calibration curve	Reference
El Tiro	ETi	Podocarpus Nat. Park, **Ec.**	2810	subpáramo	IntCal13 (LAPD-1)[a,b]	Niemann and Behling, (2008)
Lag. Pallcacocha	LPa	El Cajas Nat. Park, **Ec.**	4050	páramo	IntCal98[c]	This study and Hansen et al., 2003
Lag. Llaviucu	LLl	El Cajas Nat. Park, **Ec.**	3150	andean forest	IntCal13[a]	Nascimento et al. (2020)
Cerro Toledo	CTo	Podocarpus Nat. Park, **Ec.**	3150	páramo	CalPal 2007[d]	Brunschön and Behling, (2009)
Cayambe	Cay	Cayambe Coca Nat. Park, **Ec.**	3780	páramo	IntCal13[a,b] (LAPD-1)	Graf, (1992)
Cajanuma Valley	CVa	Podocarpus Nat. Park, **Ec.**	3285	páramo	IntCal13[a,b] (LAPD-1)	Villota and Behling, (2014)
Lag. Chorreras	LCh	El Cajas Nat. Park, **Ec.**	3700	páramo	Intcal98[c]	Hansen et al. (2003)
Lag. de la Cocha	LCo	Guamués Basin, **Col.**	2780	andean forest	IntCal09[e]	González-Carranza et al. (2012)
M772056-2	Gua	Guayaquil Bay, **Ec.**	0	marine	Marine09[e]	Seillès et al. (2015)

[a] Reimer et al., 2013.
[b] LAPD-1 = Latin American Pollen Database chronology revision by Flantua et al., 2016).
[c] Stuiver et al., 1998.
[d] Weninger et al., (2008).
[e] Reimer et al., (2009).

macro-charcoal was absent in the sediments, suggesting that the watershed of Pallcacocha was not intensively used by people, in contrast to the archaeological site density across Ecuador after 3000 cal yr BP (Fig. 2) and in broader areas in the eastern Andean flank (Sales et al., 2022). *Z. mays* pollen represent a predominantly local signal (Hofmann et al., 2014) and it is therefore likely that people attempted agriculture in the vicinity of Pallcacocha, but remained low intensity. Local intensive agriculture by the Cañari in the watershed would have resulted in high proportions of Caryophyllaceae, Amaranthaceae, *Thalictrum* sp., Poaceae, *Z. mays* and charcoal such as observed in the Lake Huila record in the northern Ecuadorian Andes (Loughlin et al., 2018). Nevertheless, people were active in the region which is revealed through the presence of *Z. mays* in Pallcacocha, Laguna Chorreras (~8 km), Laguna Llaviucu (~12 km) and archaeological records within the ECNP (Ministerio del Ambiente del Ecuador, 2018) and the surrounding region (Fig. S2) (Goldberg et al., 2016). As agricultural activity in the region began ca. 1800 cal yr BP., the synchrony between *A. acuminata* influx and El Niño-induced precipitation events became more evident in the record. Early agricultural activities seem to have amplified the impact of El Niño on the landscape at levels comparable to, but not as strong as, human amplification of the El Niño signal in Lake Sauce in the western Amazonian lowlands (Bush et al., 2017) and Laguna Llaviucu in the ECNP (Nascimento et al., 2020).

4.2. Implications

Mass movements are a pervasive geohazard in the Andes (Fig. 5). Between 1970 and 2007 C E approximately 11,000 people were killed and 38,000 homes were destroyed by debris flows and landslides in the Andes, with peaks in occurrences in Ecuador and Peru during El Niño years (Comunidad Andina, 2009). In Ecuador, 150 casualties were linked to a single mass movement event during the 1983–83 El Niño alone (Schuster et al., 2002). To provide a first order estimate of predicted mass movement occurrence with a doubling in El Niño frequency under a 1.5 °C warming scenario (Wang et al., 2017), we compared modern pollen influx of *A. acuminata* and mass movements in the Ecuadorian Andes between 1969 and 2000 C E. Approximately 34% of the ECNP area is susceptible to mass movements such as debris flows and landslides (Fig. 5) (Ministerio del Ambiente del Ecuador, 2018), but mass movement density and activity in the ECNP area is yet unknown. We therefore used data from the nearest reference site Reserva Biológica San Francisco (RBSF), 120 km south of ECNP, situated in the Ecuadorian Andes. In RBSF, a landslide/debris flow density of 12 slides km^{-2} was reported between 1969 and 2000 C E (Muenchow et al., 2012). Additional pollen data from sediments deposited between 1969 and 2000 C E in Laguna Pallcacocha (Hagemans et al., 2021) show an average pollen influx of ~1088 grains cm^2 yr^{-1} for *A. acuminata* 1969–2000 C E (Fig. S3). Projection of this data on the historical relation between binned *A. acuminata* influx and El Niño frequencies from L. Pallcacocha (Fig. 6) show that a potential future El Niño frequency of ~20 moderate to extreme events per 100 years compares to a 2–4 time higher levels of landscape disturbance as indicated by the *A. acuminata* influx rates. This projection does not take into account potential non-linearities in this relation and extension to occurrences of mass movements is therefore not yet possible with these data. Human activities in forests can further exacerbate mass movement hazards. Deforestation and conversion to pastures results in permanent reduced slope stability (Guns and Vanacker, 2013), while mass movement susceptibility significantly increases by one order of magnitude near highways (Brenning et al., 2015). Our study shows that the interaction of climatic extremes such as those associated with future El Niño intensification (Wang et al., 2017; Cai et al., 2022) and ongoing land use change (Guns and Vanacker, 2013) is likely to increase the frequency of mass movements. These aspects require further study and should consider the temporal and spatial change of human disturbance patterns and deforestation in the Andes. These combined threats not only threatens infrastructure, ecosystems and economics, but also poses

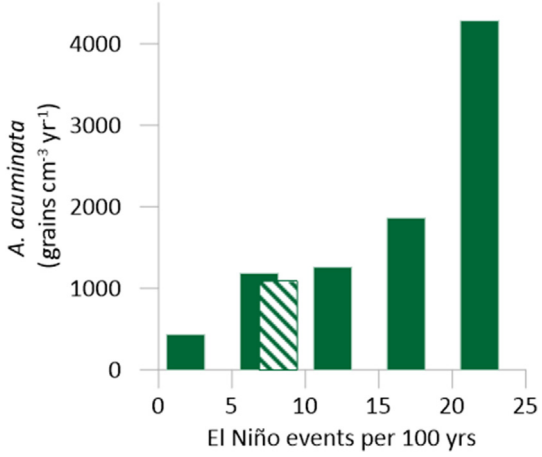

Fig. 6. Binned *A. acuminata* influx (grains cm^{-2} yr^{-1}) versus the number of El Niño events per 100 years based on the Laguna Pallcacocha laminae record (Moy et al., 2002; Rodbell et al., 1999) for 0–5, 5–10, 10–15, 15–20 and > 20 El Niño events per 100 years. Hatched bar represents the influx of *A. acuminata* pollen in the past century (Supplementary Fig. S3) versus the frequency of modern-day strong El Niño events.

an increased risk to the millions of people living in the Andes (Schoolmeester et al., 2016).

Author contributions

K. Hagemans: Formal analysis, Investigation, Visualization, Data curation, Writing - original draft and revision editing, D.H. Urrego: Investigation, Methodology, Writing - original draft and review & editing. W.D. Gosling: Investigation, Methodology, Writing - original draft and review & editing. D.T. Rodbell: Conceptualization, Investigation, Writing - review & editing.. F. Wagner-Cremer: Conceptualization, Funding acquisition, Resources, Supervision, Writing - review & editing. T.H. Donders: Conceptualization, Methodology, Visualization, Funding acquisition, Supervision, Project administration, Data curation, Writing - original draft and review & editing.

Declaration of competing interest

The authors declare that they have no known competing financial interests or personal relationships that could have appeared to influence the work reported in this paper.

Data availability

i have matached my data in the supplement

Acknowledgements

This research was funded by the Earth and Life Science council (ALW) of the Netherlands Organisation of Scientific Research (NWO) (grant number 824.14.018). Our thanks also go the Ministry of Environment of Ecuador (MAE) for providing research and fieldwork permissions (permit number 009_SGA_2015_PNC_BD_-VA_Donders). We thank W.R. Plugge for contributing to the charcoal analyses. We thank C.N.H. McMichael for advise on data analyses and H. Hooghiemstra and two anonymous reviewers for manuscript improvements and suggestion for additional sites. The work of data contributors, data stewards, and the Neotoma community and constituent Latin American Pollen Database is gratefully acknowledged.

Appendix A. Supplementary data

Supplementary data to this article can be found online at https://doi.org/10.1016/j.quascirev.2022.107762.

References

Andina, Comunidad, 2009. ATLAS de las dinámicas del territorio andino: Población y bienes expuestos a amenazas naturales. Predecan.
Bray, T.L., Echeverría, J., 2018. The inca centers of tomebamba and caranqui in northern chinchaisuyu. In: Alconini, S., Covey, R.A. (Eds.), The Oxford Handbook of the Incas. Oxford University Press, New York, pp. 159–177.
Brenning, A., Schwinn, M., Ruiz-Páez, A.P., Muenchow, J., 2015. Landslide susceptibility near highways is increased by 1 order of magnitude in the Andes of southern Ecuador, Loja province. Nat. Hazards Earth Syst. Sci. 15, 45–57. https://doi.org/10.5194/nhess-15-45-2015.
Brunschön, C., Behling, H., 2009. Late Quaternary vegetation, fire and climate history reconstructed from two cores at Cerro Toledo, Podocarpus National Park, southeastern Ecuadorian Andes. Quat. Res. 72, 388–399. https://doi.org/10.1016/j.yqres.2009.07.001.
Brunschön, C., Haberzettl, T., Behling, H., 2010. High-resolution studies on vegetation succession, hydrological variations, anthropogenic impact and genesis of a subrecent lake in southern Ecuador. Veg. Hist. Archaeobotany 19, 191–206. https://doi.org/10.1007/s00334-010-0236-4.
Bush, M.B., Correa-Metrio, A., van Woesik, R., Shadik, C.R., McMichael, C.N.H., 2017. Human disturbance amplifies amazonian El niño–southern oscillation signal. Global Change Biol. 23, 3181–3192. https://doi.org/10.1111/gcb.13608.
Cai, W., Ng, B., Wang, G., Santoso, A., Wu, L., Yang, K., 2022. Increased ENSO sea surface temperature variability under four IPCC emission scenarios. Nat. Clim. Change 12, 228–231. https://doi.org/10.1038/s41558-022-01282-z.
Clark, K.E., West, A.J., Hilton, R.G., Asner, G.P., Quesada, C.A., Silman, M.R., Saatchi, S.S., Farfan-Rios, W., Martin, R.E., Horwath, A.B., Halladay, K., New, M., Malhi, Y., 2016. Storm-triggered landslides in the Peruvian Andes and implications for topography, carbon cycles, and biodiversity. Earth Surf. Dyn. 4, 47–70. https://doi.org/10.5194/esurf-4-47-2016.
Colinvaux, P.A., Bush, M., Steinitz, K.M., Miller, M., 1997. Glacial and posglacial pollen records from the ecuadorian Andes and Amazon. Quat. Res. 48, 83–99.
Crausbay, S.D., Martin, P.H., 2016. Natural disturbance, vegetation patterns and ecological dynamics in tropical montane forests. J. Trop. Ecol. 32, 384–403. https://doi.org/10.1017/S0266467416000328.
Donders, T.H., Wagner-Cremer, F., Visscher, H., 2008. Integration of proxy data and model scenarios for the mid-Holocene onset of modern ENSO variability. Quat. Sci. Rev. 27, 571–579. https://doi.org/10.1016/j.quascirev.2007.11.010.
Duque, A., Stevenson, P.R., Feeley, K.J., 2015. Thermophilization of adult and juvenile tree communities in the northern tropical Andes. Proc. Natl. Acad. Sci. USA 112, 10744–10749. https://doi.org/10.1073/pnas.1506570112.
Faegri, K., Iversen, J., 1989. Textbook of Pollen Analysis, fourth ed. Wiley, Chichester.
Feeley, K.J., Silman, M.R., Bush, M.B., Farfan, W., Cabrera, K.G., Malhi, Y., Meir, P., Revilla, N.S., Quisiyupanqui, M.N.R., Saatchi, S., 2011. Upslope migration of Andean trees. J. Biogeogr. 38, 783–791. https://doi.org/10.1111/j.1365-2699.2010.02444.x.
Flantua, S.G.A., Blaauw, M., Hooghiemstra, H., 2016. Geochronological database and classification system for age uncertainties in Neotropical pollen records. Clim. Past 12, 387–414. https://doi.org/10.5194/cp-12-387-2016.
Foster, P., 2001. The potential impacts of global climate change on tropical montane cloud forests. Earth Sci. Rev. 55, 73–106. https://doi.org/10.1016/S0012-8252(01)00056-3.
Goldberg, A., Mychajliw, A.M., Hadly, E.A., 2016. Post-invasion demography of prehistoric humans in South America. Nature 532, 232–235. https://doi.org/10.1038/nature17176.
González-Carranza, Z., Hooghiemstra, H., Vélez, M.I., 2012. Major altitudinal shifts in Andean vegetation on the Amazonian flank show temporary loss of biota in the Holocene. Holocene 22, 1227–1241. https://doi.org/10.1177/0959683612451183.
Graf, K., 1992. Pollendiagramme aus den Anden: Eine Synthese zur Klimageschichte und Vegetationsentwicklung seit der letzten Eiszeit. University of Zurich.
Grimm, E.C., 1987. CONISS: a FORTRAN 77 program for stratigraphically constrained cluster analysis by the method of incremental sum of squares. Comput. Geosci. 13, 13–35. https://doi.org/10.1016/0098-3004(87)90022-7.
Guns, M., Vanacker, V., 2013. Forest cover change trajectories and their impact on landslide occurrence in the tropical Andes. Environ. Earth Sci. 70, 2941–2952. https://doi.org/10.1007/s12665-013-2352-9.
Hagemans, K., Tóth, C., Ormaza, M., Gosling, W.D., Urrego, D.H., 2019. Modern Pollen-Vegetation Relationships along a Steep Temperature Gradient in the Tropical Andes of Ecuador. https://doi.org/10.1017/qua.2019.4.
Hagemans, K., Nooren, K., de Haas, T., Córdova, M., Hennekam, R., Stekelenburg, M.C.A., Rodbell, D.T., Middelkoop, H., Donders, T.H., 2021. Patterns of alluvial deposition in Andean lake consistent with ENSO trigger. Quat. Sci. Rev. 259. https://doi.org/10.1016/j.quascirev.2021.106900.
Hansen, B.C.S., Rodbell, D.T., Seltzer, G.O., León, B., Young, K.R., Abbott, M., 2003. Late-glacial and Holocene vegetational history from two sites in the western Cordillera of southwestern Ecuador. Palaeogeogr. Palaeoclimatol. Palaeoecol. 194, 79–108. https://doi.org/10.1016/S0031-0182(03)00272-4.
Haslett, J., Parnell, A., 2008. A simple monotone process with application to radiocarbon-dated depth chronologies. J. R. Stat. Soc. Ser. C Appl. Stat. 57, 399–418. https://doi.org/10.1111/j.1467-9876.2008.00623.x.
Hofmann, F., Otto, M., Wosniok, W., 2014. Maize pollen deposition in relation to distance from the nearest pollen source under common cultivation - results of 10 years of monitoring (2001 to 2010). Environ. Sci. Eur. 26, 1–14. https://doi.org/10.1186/s12302-014-0024-3.
Hooghiemstra, H., 1984. Vegetational and Climatic History of the High Plain of Bogotá, Colombia: a Continuous Record of the Last 3.5 Million Years. Diss. Bot. University of Amsterdam, Amsterdam.
IPCC, 2021. In: Masson-Delmotte, V., Zhai, P., Pirani, A., Connors, S.L., Péan, C., Berger, S., Caud, N., Chen, Y., Goldfarb, L., Gomis, M.I., Huang, M., Leitzell, K., Lonnoy, E., Matthews, J.B.R., Maycock, T.K., Waterfield, T., Yelekçi, O., Yu, R., Zhou, B. (Eds.), Climate Change 2021: the Physical Science Basis. Contribution of Working Group I to the Sixth Assessment Report of the Intergovernmental Panel on Climate Change. Cambridge University Press, Cambridge, United Kingdom and New York, NY, USA. https://doi.org/10.1017/9781009157896 (in press).
Keefer, D.K., Moseley, M.E., DeFrance, S.D., 2003. A 38 000-year record of floods and debris flows in the Ilo region of southern Peru and its relation to El Niño events and great earthquakes. Palaeogeogr. Palaeoclimatol. Palaeoecol. 194, 41–77. https://doi.org/10.1016/S0031-0182(03)00271-2.
Kiefer, J., Karamperidou, C., 2019. High-resolution modeling of ENSO-induced precipitation in the tropical andes: implications for proxy interpretation. Paleoceanogr. Paleoclimatol. 34, 217–236. https://doi.org/10.1029/2018PA003423.
Loughlin, N.J.D., Gosling, W.D., Mothes, P., Montoya, E., 2018. Ecological consequences of post-Columbian indigenous depopulation in the Andean–Amazonian corridor. Nat. Ecol. Evol. 2, 1233–1236. https://doi.org/10.1038/s41559-018-0602-7.
Lozano, P., Busmann, R., Kupers, M., Diego Lozano, C., 2008. Natural landslides and pioner communities in the Mountain Ecosystems of Eastern Podocarpus

National Park | Deslizamientos naturales y comunidades pionera de ecosistemas montanos al occidente del parque nacional podocarpus (Ecuador). Caldasia 30, 1–19.
Marchant, R., Almeida, L., Behling, H., Berrio, J.C., Bush, M., Cleef, A., Duivenvoorden, J., Kappelle, M., De Oliveira, P., Teixeira de Oliveira-Filho, A., Lozano-Garćia, S., Hooghiemstra, H., Ledru, M.P., Ludlow-Wiechers, B., Markgraf, V., Mancini, V., Paez, M., Prieto, A., Rangel, O., Salgado-Labouriau, M.L., 2002. Distribution and ecology of parent taxa of pollen lodged within the Latin American Pollen Database. Rev. Palaeobot. Palynol. 121, 1–75. https://doi.org/10.1016/S0034-6667(02)00082-9.
McPhaden, M.J., Zebiak, S.E., Glantz, M.H., 2006. ENSO as an integrating concept in earth science. Science 84 314, 1740–1745. https://doi.org/10.1126/science.1132588.
Ministerio del Ambiente del Ecuador, 2018. Actualización del plan de manejo del Parque Nactional Cajas.
Ministerio del Ambiente Ecuador (MAE), 2014. Mapa de cobertura y uso de la tierra del 2014. Sistema Nacional de Monitoreo del Patrimonio Natural. MAE, Quito, Ecuador.
Moreiras, S.M., 2005. Climatic effect of ENSO associated with landslide occurrence in the central andes, mendoza province, Argentina. Landslides 2, 53–59. https://doi.org/10.1007/s10346-005-0046-4.
Moy, C.M., Seltzer, G.O., Rodbell, D.T., Anderson, D.M., 2002. Variability of El niño/southern oscillation activity at millennial timescales during the holocene epoch. Nature 420, 162–165. https://doi.org/10.1038/nature01194.
Muenchow, J., Brenning, A., Richter, M., 2012. Geomorphic process rates of landslides along a humidity gradient in the tropical Andes. Geomorphology 139–140, 271–284. https://doi.org/10.1016/j.geomorph.2011.10.029.
Myers, N., Mittermeier, R.A., Mittermeier, C.G., da Fonseca, G.A.B., Kent, J., 2000. Biodiversity hotspots for conservation priorities. Nature 403, 853–858. https://doi.org/10.1038/35002501.
Nascimento, M.N., Mosblech, N.A.S., Raczka, M.F., Baskin, S., Manrique, K.E., Wilger, J., Giosan, L., Benito, X., Bush, M.B., 2020. The adoption of agro-pastoralism and increased ENSO frequency in the Andes. Quat. Sci. Rev. 243, 106471. https://doi.org/10.1016/j.quascirev.2020.106471.
Niemann, H., Behling, H., 2008. Late Quaternary vegetation, climate and fire dynamics inferred from the El Tiro record in the southeastern Ecuadorian Andes. J. Quat. Sci. 23, 203–212. https://doi.org/10.1002/jqs.
Niemann, H., Brunschön, C., Behling, H., 2010. Vegetation/modern pollen rain relationship along an altitudinal transect between 1920 and 3185 m a.s.l. in the Podocarpus National Park region, southeastern Ecuadorian Andes. Rev. Palaeobot. Palynol. 159, 69–80. https://doi.org/10.1016/j.revpalbo.2009.11.001.
Ohl, C., Bussmann, R., 2004. Recolonisation of natural landslides in tropical mountain forests of Southern Ecuador. Feddes Repert. 115, 248–264. https://doi.org/10.1002/fedr.200311041.
Olivera, M.M., Duivenvoorden, J.F., Hooghiemstra, H., 2009. Pollen rain and pollen representation across a forest-páramo ecotone in northern Ecuador. Rev. Palaeobot. Palynol. 157, 285–300. https://doi.org/10.1016/j.revpalbo.2009.05.008.
Paolini, L., Villalba, R., Ricardo Grau, H., 2005. Precipitation variability and landslide occurrence in a subtropical mountain ecosystem of NW Argentina. Dendrochronologia 22, 175–180. https://doi.org/10.1016/j.dendro.2005.06.001.
Pérez-Escobar, O.A., Zizka, A., Bermúdez, M.A., Meseguer, A.S., Condamine, F.L., Hoorn, C., Hooghiemstra, H., Pu, Y., Bogarín, D., Boschman, L.M., Pennington, R.T., Antonelli, A., Chomicki, G., 2022. The Andes through time: evolution and distribution of Andean floras. Trends Plant Sci. 27, 364–378. https://doi.org/10.1016/j.tplants.2021.09.010.
Reese, C.A., Liu, K.B., 2005. A modern pollen rain study from the central Andes region of South America. J. Biogeogr. 32, 709–718. https://doi.org/10.1111/j.1365-2699.2005.01183.x.
Reimer, P.J., Baillie, M.G.L., Bard, E., Bayliss, A., Beck, J.W., Blackwell, P.G., Bronk Ramsey, C., Buck, C.E., Burr, G.S., Edwards, R.L., Friedrich, M., Grootes, P.M., Guilderson, T.P., Hajdas, I., Heaton, T.J., Hogg, A.G., Hughen, K.A., Kaiser, K.F., Kromer, B., McCormac, F.G., Manning, S.W., Reimer, R.W., Richards, D.A., Southon, J.R., Talamo, S., Turney, C.S.M., van der Plicht, J., Weyhenmeyer, C.E., 2009. IntCal09 and Marine09 radiocarbon age calibration curves, 0-50,000 years cal BP. Radiocarbon 51 (4), 1111–1150.
Reimer, P.J., Bard, E., Bayliss, A., Beck, J.W., Blackwell, P.G., Bronk Ramsey, C., Grootes, P.M., Guilderson, T.P., Haflidason, H., Hajdas, I., Hatt'e, C., Heaton, T.J., Hoffmann, D.L., Hogg, A.G., Hughen, K.A., Kaiser, K.F., Kromer, B., Manning, S.W., Niu, M., Reimer, R.W., Richards, D.A., Scott, E.M., Southon, J.R., Staff, R.A., Turney, C.S.M., van der Plicht, J., 2013. IntCal13 and Marine13 radiocarbon age calibration curves 0-50,000 Years cal BP. Radiocarbon 55 (4), 1869–1887.
Richter, M., 2009. To what extent do natural disturbances contribute to Andean plant diversity? A theoretical outline from the wettest and driest parts of the tropical Andes. Adv. Geosci. 22, 95–105. https://doi.org/10.5194/adgeo-22-95-2009.
Rodbell, D.T., Seltzer, G.O., Anderson, D.M., Abbott, M.B., Enfield, D.B., Newman, J.H., 1999. An ~15,000-year record of El Niño-driven alluviation in southwestern Ecuador. Science 80 (283), 516–520. https://doi.org/10.1126/science.283.5401.516.
Rodbell, D.T., Bagnato, S., Nebolini, J.C., Seltzer, G.O., Abbott, M.B., 2002. A late glacial-holocene tephrochronology for glacial lakes in southern Ecuador. Quat. Res. 57, 343–354. https://doi.org/10.1006/qres.2002.2324.
Sales, R.K., McMichael, C.N.H., Flantua, S.G.A., Hagemans, K., Zondervan, J.R., González-Arango, C., Church, W.B., Bush, M.B., 2022. Potential distributions of pre-Columbian people in Tropical Andean landscapes. Phil.Trans. R. Soc. B 377, 20200502. https://doi.org/10.1098/rstb.2020.0502.
Schiferl, J.D., Bush, M.B., Silman, M.R., Urrego, D.H., 2018. Vegetation responses to late Holocene climate changes in an Andean forest. Quat. Res. 1–15. https://doi.org/10.1017/qua.2017.64.
Schneider, C.A., Rasband, W.S., Eliceiri, K.W., 2012. NIH Image to ImageJ: 25 years of image analysis. Nat. Methods 9 (7), 671–675. https://doi.org/10.1038/nmeth.2089.
Schneider, T., Hampel, H., Mosquera, P.V., Tylmann, W., Grosjean, M., 2018. Paleo-ENSO revisited: Ecuadorian Lake Pallcacocha does not reveal a conclusive El Niño signal. Global Planet. Change 168, 54–66. https://doi.org/10.1016/j.gloplacha.2018.06.004.
Schoolmeester, T., Saravia, M., Andresen, M., Postigo, J., Valverde, A., Jurek, M., Alfthan, B., Giada, S., 2016. Outlook on climate change adaptation in the Tropical Andes mountains. Mountain Adaptation Outlook Series. Nairobi, Arendal, Vienna and Lima 1–94.
Schuster, R.L., Salcedo, D.A., Valenzuela, L., 2002. Overview of catastrophic landslides of South America in the twentieth century. Rev. Eng. Geol. 15, 1–34.
Seillès, B., Sánchez Goñi, M.F., Ledru, M.P., Urrego, D.H., Martinez, P., Hanquiez, V., Schneider, R., 2015. Holocene land–sea climatic links on the equatorial Pacific coast (Bay of Guayaquil, Ecuador). Holocene 26, 567–577. https://doi.org/10.1177/0959683615612566.
Sepúlveda, S.A., Rebolledo, S., Vargas, G., 2006. Recent catastrophic debris flows in Chile : geological hazard , climatic relationships and human response. Quat. Int. 158, 83–95. https://doi.org/10.1016/j.quaint.2006.05.031.
Stockmarr, J., 1971. Tablets with spores used in absolute pollen analysis. Pollen et Spores XIII 615–621.
Stuiver, M., Reimer, P.J., Bard, E., Beck, J.W., Burr, G.S., Hughen, K.A., Kromer, B., McCormac, G., der Plicht, V.J., Spurk, M., 1998. INTCAL98 radiocarbon age calibration, 24,000-0 cal BP. Radiocarbon 40 (3), 1041–1083.
Thompson, D.M., Conroy, J.L., Collins, A., Hlohowskyj, S.R., Overpeck, J.T., Riedinger-Whitmore, M., Cole, J.E., Bush, M.B., Whitney, H., Corley, T.L., Kannan, M.S., 2017. Tropical pacific climate variability over the last 6000 years as recorded in bainbridge crater lake, galápagos. Paleoceanography 32, 903–922. https://doi.org/10.1002/2017PA003089.
Urrego, D.H., Silman, M.R., Bush, M.B., 2005. The last glacial maximum: stability and change in a western amazonian cloud forest. J. Quat. Sci. 20, 693–701. https://doi.org/10.1002/jqs.976.
NASA Shuttle Radar Topography Mission (SRTM), Version 3.0., Global 1 arc second, region: South America, USGS, Reston, 2014.
Urrego, D.H., Niccum, B.A., La Drew, C.F., Silman, M.R., Bush, M.B., 2011a. Fire and drought as drivers of early Holocene tree line changes in the Peruvian Andes. J. Quat. Sci. 26, 28–36. https://doi.org/10.1002/jqs.1422.
Urrego, D.H., Silman, M.R., Correa-Metrio, A., Bush, M.B., 2011b. Pollen-vegetation relationships along steep climatic gradients in western Amazonia. J. Veg. Sci. 22, 795–806. https://doi.org/10.1111/j.1654-1103.2011.01289.x.
van Geel, B., Gelorini, V., Lyaruu, A., Aptroot, A., Rucina, S., Marchant, R., Damsté, J.S.S., Verschuren, D., 2011. Diversity and ecology of tropical African fungal spores from a 25,000-year palaeoenvironmental record in southeastern Kenya. Rev. Palaeobot. Palynol. 164, 174–190. https://doi.org/10.1016/j.revpalbo.2011.01.002.
Villota, A., Behling, H., 2014. Late glacial and holocene environmental change inferred from the páramo of cajanuma in the podocarpus national park, Southern Ecuador. Caldasia 36, 345–364. https://doi.org/10.15446/caldasia/v36n2.47491.
Vuille, M., Bradley, R.S., Keimig, F., 2000. Climate variability in the andes of Ecuador and its relation to tropical pacific and atlantic sea surface temperature anomalies. J. Clim. 13, 2520–2535. https://doi.org/10.1175/1520-0442(2000)013<2520:CVITAO>2.0.CO;2.
Wang, G., Cai, W., Gan, B., Wu, L., Santoso, A., Lin, X., Chen, Z., McPhaden, M.J., 2017. Continued increase of extreme El Niño frequency long after 1.5 °C warming stabilization. Nat. Clim. Change 7, 568–572. https://doi.org/10.1038/nclimate3351.
Weng, C., Bush, M.B., Chepstow-Lusty, A.J., 2004a. Holocene changes of Andean alder (Alnus acuminata) in highland Ecuador and Peru. J. Quat. Sci. 19, 685–691. https://doi.org/10.1002/jqs.882.
Weng, C., Bush, M.B., Silman, M.R., 2004b. An analysis of modern pollen rain on an elevational gradient in southern Peru. J. Trop. Ecol. 20, 113–124. https://doi.org/10.1017/S0266467403001068.
Weninger, B., Jöris, O., Danzeglocke, U., 2008. CalPal-2007. Cologne Radiocarbon Calibration & Palaeoclimate Research Package. University of Cologne. http://www.calpal.de/.
White, S.M., Ravelo, A.C., Polissar, P.J., 2018. Dampened El Niño in the early and mid-holocene due to insolation-forced warming/deepening of the thermocline. Geophys. Res. Lett. 45, 316–326. https://doi.org/10.1002/2017GL075433.
Williams, J.W., Grimm, E.C., Blois, J.L., Charles, D.F., Davis, E.B., Goring, S.J., Graham, R.W., Smith, A.J., Anderson, M., Arroyo-Cabrales, J., Ashworth, A.C., Betancourt, J.L., Bills, B.W., Booth, R.K., Buckland, P.I., Curry, B.B., Giesecke, T., Jackson, S.T., Latorre, C., Nichols, J., Purdum, T., Roth, R.E., Stryker, M., Takahara, H., 2018. The Neotoma Paleoecology Database, a multiproxy, international, community-curated data resource. Quat. Res. 89, 156–177. https://doi.org/10.1017/qua.2017.105.